scientific reports

Check for updates

OPEN

Oligomeric hyaluronic acid-modified liposomes effectively improved skin permeability and anti-ageing activity of ellagic acid

Xiaojing Yang[1], Kaiyuan Miao[1], Zhiwei Chen[1], Yan Meng[1,4], Jie Xiang[3], Chiqing Chen[3]✉, Xinyan Chen[1,4]✉ & Zhaohua Shi[2,4]✉

To overcome natural skin barrier, deliver ellagic acid (EA) to the dermis, and promote its anti-ageing efficacy, oligomeric hyaluronic acid (HA) modified EA-loaded liposomes (EA-HA-L) were constructed via self-synthesized different molecular weights of HA linked cholesterol (HA-Chol), and then the effect of HA molecular weight on the skin permeability of EA was explored to clarify the optimal molecular weight of HA with best transdermal delivery effectiveness. Finally, a series of in vitro and in vivo experiments were conducted to survey the transdermal mechanism, skin irritation, antioxidant, anti-photo ageing and antiwrinkle effects of EA-loaded liposomes modified with the optimal molecular weight of HA. The results showed that EA-HA-L had less than 200 nm particle size and high encapsulation efficiency. Among them, 5 kDa of oligomeric HA-modified liposomes (EA-HA5k-L) maximized the skin penetration and retention of EA and promoted the distribution width of EA in the skin far beyond the thickness of the epidermal layer, indicating its good ability to deliver EA to the dermis. EA-HA5k-L displayed uniformly sized nanosphere morphology and slow-release behavior in neutral and acidic environments that simulated skin. The transdermal mechanism of EA-HA5k-L was proven to be related to the loosening of the stratum corneum, reduction of calcium adhesion proteins, and recognition of CD44 receptor. EA-HA5k-L had no irritant effect on the chicken embryo chorioallantoic membrane, with an irritant index close to 0.9% NaCl. EA-HA5k-L not only improved the clearance rate of EA on DPPH and hydroxyl radicals but also elevated its inhibition effect on elastase. Significantly, compared to free EA and EA-loaded liposomes without oligomeric HA modification (EA-L), EA-HA5k-L significantly increased the cellular uptake of EA through receptor-mediated endocytosis, and effectively blocked the increase in metalloproteinase-1 (MMP-1) content and decrease in type I collagen content induced by UVB in human dermal fibroblasts (HDFs), demonstrating better anti-photo ageing effectiveness. Moreover, EA-HA5k-L upregulated the relative expression of the elastin gene and three types of type I collagen gene (col1a1a, col1a1b, and col1a2) in zebrafish, and its expression promotion rates in col1a1b, col1a2 and elastin were remarkably higher than those of free EA, EA-L, and acetyl hexapeptide-8 as positive control. Conclusively, EA-HA5k-L ameliorated the anti-ageing effectiveness of EA due to the successful transdermal delivery and efficient cellular uptake, and 5 kDa of oligomeric HA-modified liposomes may be a promising transdermal delivery carrier to overcome skin barrier and upgrade the application prospects of EA in anti-skin ageing.

Keywords Ellagic acid, Hyaluronic acid-modified cholesterol, Liposomes, Skin permeability, Anti-ageing

Human skin ageing is caused by internal time accumulation (endogenous ageing) and external environmental exposure (exogenous ageing), such as photo-ageing caused by prolonged exposure to ultraviolet light. Endogenous and exogenous ageing eventually leads to the loss of the skin's physiological functions, which increases the risk of various diseases due to reduced production of antioxidant, oxidative damage, inflammatory reactions and the production of matrix metalloproteinases, the collagen and elastin content in the dermis decreases, leading to

[1]School of Pharmacy, Hubei University of Chinese Medicine, Wuhan 430065, China. [2]Key Laboratory of Resource and Chinese Medicine Compounding, Ministry of Education, Hubei University of Chinese Medicine, Wuhan 430065, China. [3]Wufeng Chicheng Biotech Co., Ltd, Yichang 443400, China. [4]Hubei Shizhen Laboratory, Wuhan 430065, China. ✉email: 153670858@qq.com; chenxy_328@163.com; zhshi78@hbucm.edu.cn

skin ageing, structural damage and the formation of wrinkles. Some functional ingredients have been proven to prevent skin ageing. For example, salicylic acid is an organic acid widely used in cosmetics, which can penetrate pores, dissolve ageing keratin to form new cells, enhance skin cell metabolism, and to some extent prevent ultraviolet damage and photoaging. However, improper or incorrect dosage can excessively stimulate the skin and damage the normal stratum corneum[1]. 4-methylbenzylidene camphor (4-MBC) is an organic camphor derivative that can delay skin ageing by resisting UVB radiation. Unfortunately, 4-MBC may affect the secretion of thyroid and estrogen systems, and long-term use may lead to certain risks[2].

Currently, based on the concept of returning to nature, searching for natural, green, and environmentally friendly active ingredients from plants or food as cosmetic ingredients has become a new trend. Numerous studies have confirmed that natural polyphenols play a beneficial role in preventing skin ageing. EA is a naturally occurring polyphenolic compound found primarily in fruits, nuts and Galla chinensis[3,4]. EA is often used as a dietary supplement for treating cancer and other diseases in the U.S., Europe and other countries[5]. Not only that, it has been proven that EA also has excellent anti-inflammatory, antioxidant, whitening, anti-photoageing and anti-ageing effects, making it a promising natural cosmetic ingredient[6,7]. However, EA is a polyphenol dilactone with a unique structure that results in abysmal water solubility, lipid solubility, and skin permeability. Due to the oil–water distribution coefficient (LogP) of only 0.52, it is difficult for EA to penetrate the dense stratum corneum[8]. Besides, some proteins related to skin elasticity, such as collagen and elastin, are mainly expressed in the dermis below the dense stratum corneum. Therefore, it is necessary to construct a percutaneous delivery system to address these issues and enhance the application value of EA in anti-ageing.

Liposomes are nanocarriers composed of phospholipids and cholesterol with a phospholipid bilayer structure. Its particular phospholipid bilayer structure can better penetrate the cellular space of the stratum corneum and promote the transdermal absorption of loaded drugs. Hence, liposome technology has been applied in cosmetics to increase the solubility and transdermal effect of insoluble active ingredients[9–11]. Nevertheless, recent research has found that conventional liposomes face difficulties delivering drugs to the dermis, as the loaded drugs are usually blocked in the stratum corneum or epidermis[12]. Hyaluronic acid (HA) is a natural anionic mucopolysaccharide with good biocompatibility and biodegradability. It has been proven to be an excellent transdermal enhancer, especially for low molecular weight HA, with a better transdermal promotion effect. However, it is still unclear how low the molecular weight of HA is required to deliver drugs to the dermis.

Given the above, to overcome the natural skin barrier, deliver ellagic acid (EA) to the dermis, and optimize its anti-ageing efficacy, we fabricated oligomeric HA-modified EA-loaded liposomes (EA-HA-L) via self-synthesized different molecular weights of HA linked cholesterol (Fig. 1), and then explored the effect of HA molecular weight on the skin permeability of EA. Finally, we evaluated the transdermal mechanism, skin irritation, antioxidant, anti-photo ageing and antiwrinkle effects of EA-loaded liposomes modified with the optimal molecular weight of HA through rat skin, chicken embryo chorioallantoic membrane, UVB-induced fibroblasts, and Zebrafish.

Materials and methods

Materials

EA (purity ≥ 98%) was provided by Wufeng Chicheng Biotechnology Co., Ltd (Yichang, China). EA standard (purity ≥ 98%) was bought from Shanghai Yuanye Biotechnology Co., Ltd (Shanghai, China). Soy phospholipid (purity ≥ 95%) was purchased from AVT (Shanghai) Pharmaceutical Tech Co., Ltd (Shanghai, China). Cholesterol

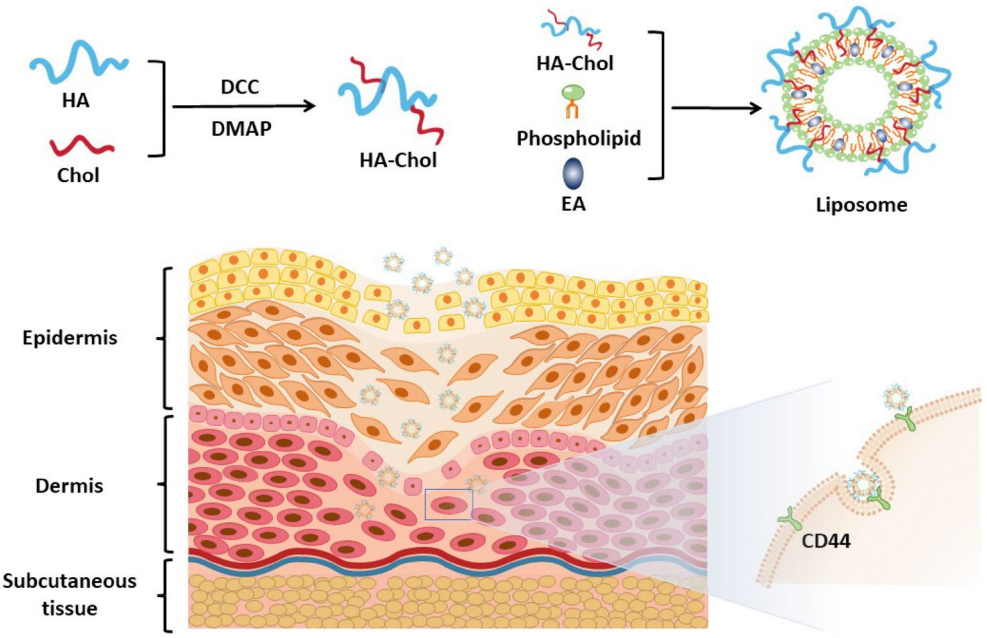

Fig. 1. Synthesis of HA-Chol, construction of EA-HA-L and transdermal delivery of EA-HA-L.

(purity ≥ 98%) was bought from Solarbio Science & Technology Co., Ltd (Beijing, China). Hyaluronic acid with molecular weight 0.8 kDa, 5 kDa, and 52 kDa, respectively, were supplied by Bloomage Biotechnology Co., Ltd (Beijing, China). 2,2-Diphenyl-1-picrylhydrazyl (DPPH), N-succinyl-Ala-Ala-Ala-p-nitroanilide (NAAAPN), and elastase were all purchased from Shanghai Macklin Biochemical Technology Co., Ltd (Shanghai, China). All other chemicals were analytically pure. Ultrapure water was generated using a Milli-Q system (Millipore, Bedford, USA).

Cell lines and culture

Human dermal fibroblasts (HDFs) were obtained from Wuhan Yuansheng Primary Biomedical Technology Co., Ltd. (Wuhan, China) and grown in Dulbecco® improved Eagle medium containing 10% fetal bovine serum (FBS) and 1% penicillin–streptomycin. The cells were cultured in a humidified incubator filled with 5% CO_2 at a temperature of 37 °C.

Animals

The male Sprague Dawley rats weighing about 150–160 g were obtained from Wuhan Zikeheng Biotechnology Co., Ltd (Wuhan, China). Zebrafish developed to the sixth day were selected as experimental organisms. All the animal experiments were performed in accordance with the Guide for Care and Use of Laboratory Animals approved by Hubei University of Chinese Medicine. Also, experiments were done in accordance with the approved protocols, institutional guidelines for the care and use of laboratory animals and ARRIVE recommendations.

Preparation and characterization of EA-HA-L

Different molecular weights of oligomeric HA-modified EA-loaded liposomes (EA-HA0.8 k-L, EA-HA5k-L, EA-HA52k-L) were prepared by thin-film hydration method combined with sonication. The lipid mixture of 4 mg EA and 160 mg soy phospholipid was dissolved in tetrahydrofuran and then evaporated at 30 °C by rotary evaporation to form a thin film on the wall of a 250 mL flask. The lipid thin film was hydrated with 10 mL ultrapure water containing 16 mg cholesterol modified with different molecular weights of oligomeric HA (HA0.8 k-Chol, HA5k-Chol or HA52k-Chol), respectively. The liposome dispersion was subsequently subjected to sonication at 262 W for 21 min in an ice-water bath for downsizing. The prepared liposomes were stored at 4 °C prior to use. As controls, EA-loaded liposomes without oligomeric HA modification (EA-L) and oligomeric HA-modified liposomes without loading EA (HA-L) were prepared via similar methods as described above, except that cholesterol was dissolved together with EA and soy phospholipid in tetrahydrofuran.

The particle size, PDI, and Zeta potential of the prepared liposomes were determined by the Malvern particle size meter (Nano ZS90, Malvern, England). The encapsulation efficiency of EA was calculated according to the literature method[13].

Skin penetration and retention analysis

A 3% sodium pentobarbital solution (100 mg/kg body weight) was administered via intraperitoneal injection. Using a sterilized 1 mL syringe, the rat was restrained in a supine position, and the abdomen was disinfected. The needle was inserted at a 45° angle to a depth of 0.5–1 cm. After confirming no blood or fluid reflux, the solution was injected slowly. Death was confirmed by cessation of respiration and heartbeat, along with loss of corneal reflex. The experimental skins were taken from the abdomen of rats. After removing the subcutaneous fat, the skins were stored at − 80 °C until utilization. During the skin permeability experiment, the skin was sandwiched between the donor and acceptor compartments of the Franz diffusion cell, with the stratum corneum facing the donor compartment, and the diffusion area was 0.636 cm^2. The acceptor phase in the acceptor compartment was a mixed solution of methanol and saline with a volume ratio of 1:1, which was maintained at a constant temperature of 37 ± 0.5 °C and stirred throughout the entire experimental process. 2 mL of freshly made sample solution was loaded into the donor compartment and spread over the skin. Except for EA which was directly dissolved in solvent by stirring, all other samples including EA-L, EA-HA0.8k-L, EA-HA5k-L, and EA-HA52k-L were prepared using the thin-film dispersion method combined with sonication. To ensure consistent dosing across all groups, all final sample solutions were uniformly diluted to a concentration of 400 μg/mL. Then, 0.7 mL of solution was taken from the acceptor compartment at appointed intervals (1, 2, 3, 4, 6, 8, 10, 12, and 24 h) and replaced by the same volume of fresh acceptor phase to maintain a constant volume. The concentration of EA was analyzed using high-performance liquid chromatography (HPLC) (1200, Agilent, USA).

At the end of the above skin permeability test, the skin was removed from the Franz diffusion cell and washed with saline to remove the remaining sample solution. The skin was cut into small pieces and homogenized in 1 mL of methanol. The homogenized methanol solution was vortex mixed and then centrifuged at 12,000 rpm for 10 min. The residue was re-extracted once with 0.5 mL of methanol according to the above operation. After two centrifugations, the supernatant was collected, and mixed well, and the volume was 2 mL. The amount of EA in the supernatant was analyzed by HPLC.

Distribution of EA in the skin

Consistent with the methodology used in the skin penetration and retention analysis, the rat skin was incubated with 2 mL of different sample solutions in a Franz diffusion cell for 24 h. Next, the skin was washed with saline, dried with filter paper, and then cut into pieces of about 1 cm^2. After fixing with liquid nitrogen, the skin was cut into thin slices using a microtome blade and adhered to the glass slide. Finally, the distribution of EA in the skin was observed by confocal laser scanning microscopy (Eclipse Ti, Nikon, Japan).

Microscopic morphology and in vitro release behaviour of EA-HA5k-L

The morphological characterization of liposomes was analyzed by transmission electron microscopy (TEM) (JEM-1400, JEOL, Japan). The in vitro release profile of EA-loaded liposomes was monitored using a dialysis method. In brief, 2 mL of sample solution was placed in a dialysis bag (MWCO 3500) and then immersed into a 100 mL release medium composed of phosphate-citric acid buffer with pH values set to 5.5 or 7.4. The release medium was heated to 37 °C with constant agitation. At a specific time (0.5, 1, 2, 4, 6, 8, 10, 12, 24, 36, and 48 h), 1 mL of release medium was taken and replaced with the same fresh medium. The amount of EA in the release medium was measured via HPLC. The accumulative release amount of EA was calculated according to Xiao's method[13].

Study of transdermal mechanism

Skin administration

After removing the hair on the back of SD rats weighing 150–160 g, the back skin of rats was evenly divided into four administration areas (control group area, free EA area, EA-L area, and EA-HA5k-L area) and circular filter paper with a diameter of 1 cm was placed on each of the four areas. The sample solutions with the same EA concentration were added dropwise to completely moisten the filter paper, respectively. The filter paper wetted by the sample solution was covered with a sterile dressing film to avoid drug loss. After 12 h, the rats were executed, and the skin in the administration area was taken immediately for subsequent stratum corneum observation, hematoxylin and eosin (H&E) staining and immunohistochemical analysis of E-cadherin protein.

Stratum corneum ultrastructure

The rat skin treated with sample solutions was immersed in saline, cleaned, cut into suitable sizes, and fixed with 2.5% glutaraldehyde. After rinsing in phosphate buffer, the skin was fixed in 1% osmium acid, dehydrated in different volume concentrations of ethanol, and finally dried at the critical point of CO_2. The dried skin samples were placed under an ion-sputtering apparatus, and metal particles were sputtered onto the surface of the skin samples to form a layer of the metal film. The ultrastructure of the transverse and longitudinal sections of the stratum corneum was observed under a scanning electron microscope (SU8100, Hitachi, Japan).

H&E-stained and immunohistochemical analysis of skin tissues

The rat back skin treated with sample solutions was cut into long strips of 0.5 cm × 1 cm and then rinsed with saline to remove blood stains, fixed in 4% paraformaldehyde, sectioned in paraffin, stained with H&E, and finally observed under a light microscope (Eclipse E100, Nikon, Japan).

The immunohistochemical analysis of E-cadherin in the rat skin was conducted according to the literature methods[14,15]. Briefly, PBS solution containing 3% bovine serum albumin (BSA) was added dropwise to the sections and closed for 30 min at room temperature, and then incubated with E-cadherin (GB12083, Wuhan Servicebio Technology CO., LTD, China) primary antibody overnight at 4 °C. The following day, sections were treated with HRP goat anti-mouse IgG (GB23301, Wuhan Servicebio Technology CO., LTD, China) for 60 min at room temperature. Subsequently, slides were counterstained with hematoxylin and observed under a light microscope.

Skin irritation test of EA-HA5k-L

The Hen's Egg Test-Chorioallantoic Membrane (HET-CAM) was adopted to evaluate the skin irritation of EA-HA5k-L[16]. Briefly, 300 μL of liposome solution was added onto the chorioallantoic membrane of a fertilized chicken egg to monitor any hemorrhage, vasoconstriction, and coagulation phenomena occurring within the first 5 min after addition. 0.1 M NaOH was used as the positive control, and 0.9% NaCl was used as a negative control.

The irritation index (IS) was calculated by the sum of the scores of each injury according to the following equation:

$$\mathrm{IS} = \frac{(301 - \sec \mathrm{H}) \times 5}{300} + \frac{301 - \sec \mathrm{L} \times 7}{300} + \frac{301 - \sec \mathrm{C} \times 9}{300} \quad (1)$$

The secH, secL and secC represented the hemorrhage time, vessel lysis time and coagulation time, respectively.

The irritancy of the formulations was classified according to the expression: non-irritation: IS < 1; weak irritation: 1 ≤ IS < 5; moderate irritation: 5 ≤ IS < 10; obvious irritation: IS ≥ 10.

In vitro antioxidant activity of EA-HA5k-L

The scavenging activity of EA-HA5k-L against hydroxyl and DPPH radicals was used to evaluate the antioxidant ability of EA-HA5k-L. Firstly, the EA concentration of EA, EA-L, EA-HA5k-L and HA5k-L groups was set within the 50 ~ 400 μg/mL range. Next, 50 μL of sample solutions with different EA concentrations were sequentially mixed with 25 μL $FeSO_4$ (9 mM), 50 μL salicylic acid (9 mM) and 50 μL H_2O_2 (4.4 mM) in 96-well plates. After mixing evenly, the 96-well plates were kept at 37 °C for 60 min. Finally, the absorbance of each well at 510 nm was surveyed by a microplate reader (xMark™, Bio-Rad, USA) to calculate the hydroxyl free radical scavenging rate.

Similarly, 100 μL of sample solutions with different EA concentrations were mixed with 100 μL of 0.2 mM DPPH ethanol solution in 96-well plates. After mixing uniformly, the 96-well plates were left in the dark for 30 min at 25 °C, and then the absorbance of each well at 517 nm was recorded to calculate the DPPH free radical scavenging rate.

The above experiments were done in triplicate, and the average value was adopted.

Elastase inhibition activity of EA-HA5k-L

In a 96-well plate, 50 μL of sample solutions (EA, EA-L, EA-HA5k-L and HA5k-L) with different EA concentrations were mixed with 25 μL of elastase solution and 100 μL of Tris–HCL buffer (pH 8.2) sequentially, and then incubated at 25 °C for 20 min. After that, 25 μL of NAAAPN as substrate was added to each well, and the absorbance of each well at 405 nm (marked by A) was immediately measured after mixing the well. The absorbance of each well at the same wavelength (marked by A′) was measured again after incubation at 25 °C for 10 min. The difference in absorbance between each test group ΔA (A′—A) was calculated to analyze the enzyme inhibition effect of each group. The elastase inhibition rate was calculated according to the following formula. Three replicates were made for each concentration of sample solutions.

$$\text{Inhibition rate} = \left(1 - \frac{\Delta A1 - \Delta A0}{\Delta A2}\right) \times 100\% \quad (2)$$

where ΔA1 is the absorbance difference of the test group, ΔA2 is the absorbance difference of the blank control group, and ΔA0 is the absorbance difference of the sample control group.

Cell viability assay

The CCK8 method was used to assess the cytotoxicity of sample solutions at different EA concentrations (2.5, 5, 10, 20, 40 μg/mL) to HDFs. The cells were incubated with different sample solutions for 24 h in 96-well plates. After that, the cells were washed with PBS to remove residual sample solutions. 100 μL of CCK8 reagent was added to each well, and then the absorbance of the solution was determined at a wavelength of 450 nm via a microplate reader.

Cellular uptake

The HDFs were seeded in 6-well plates at a density of 2.0×10^5 cells per well. After incubation for 24 h, the cells were treated with EA, EA-L, and EA-HA5k-L at the same EA concentration for 4 h, respectively. To further survey the effect of the CD44 receptor recognition on the cellular uptake of EA, the cells in each well were preincubated with 5 mg/mL of 5 kDa HA solution for 1 h before treatment with EA, EA-L, and EA-HA5k-L. After treatment, the culture medium was removed, and the cells were washed twice with PBS and then fixed in PBS with 4% paraformaldehyde for 10 min. Finally, the cells were observed using an inverted fluorescence microscope (Olympus IX73, Olympus, Japan).

Anti-photoaging effect on human dermal fibroblasts

HDFs were seeded in 96-well plates at a density of 1.0×10^5 cells per well and incubated with different sample solutions (EA, EA-L, EA-HA5k-L and HA5k-L) at an EA concentration of 40 μg/mL for 24 h. After removing the culture medium, the cells were rinsed with PBS, irradiated with UVB (60 mJ/cm^2) in PBS for 15 min, and then further cultured with a culture medium containing FBS for 24 h. The supernatant in each well was collected, and MMP-1 content was determined using a Matrix Metalloproteinase kit (Cusabio Technology LLC). The cells without UVB irradiation were used as the control group. In contrast, the cells that were only irradiated but not treated with different sample solutions were used as the model group.

Type I collagen content was assayed according to the instructions of the Human Type I Collagen Enzyme-Linked Immunoassay Kit (Shanghai Enzyme Linked Biotechnology Co., Ltd). HDFs were seeded in 96-well plates and then treated with different sample solutions for 24 h before UVB irradiation (60 mJ/cm^2). After UVB irradiation for 15 min, the content of type I collagen in the cell supernatants was determined according to the instructions for the type I collagen kit[17].

Zebrafish experiment

Maximum tolerance concentration (MTC) of Zebrafish

Zebrafish embryos developed to the sixth day were selected as the experimental organisms. Based on the pre-test results, the EA administration concentration of different sample solutions was set at 0.625, 1.25, 2.5, 5, 10, 20 and 40 g/L. Each EA sample solution was assigned 20 zebrafish embryos, which grew in a 96-well plate (1 embryo per well). After zebrafish embryos were incubated with different concentrations of EA sample solutions in a constant temperature incubator at 28.5 ± 0.5 °C for 48 h, the death and malformation status of zebrafish were observed and recorded. The MTC values were determined based on the concentration of EA that did not cause zebrafish death or malformation.

Type I collagen and elastin gene expression

This experiment was performed following methods as previously reported[18]. 5 mL of sample solution with an EA concentration of 2.5 g/L was added to a 96-well plate where zebrafish embryos lived. After incubation for 24 h, total RNA extraction, reverse transcription, and fluorescence quantitative PCR (QuantStudio 5, Applied Biosystems, USA) were performed on each group of zebrafish. The β-actin gene was used as the internal reference gene, and the relative expression level of the type I collagen gene and elastin gene in each group was calculated. The gene expression promotion rate of the test group was calculated by comparing it with the control group. Acetyl Hexapeptide-8 was chosen as a positive control, and three biological replicates were set up with 10 fish in each replicate. The primer sequences are listed in Table 1.

Primer name	Primer sequence
β-actin forward primer	5′-GCTGACAGGATGCAGAAGGA-3′
β-actin reverse primer	5′-TAGAAGCATTTGCGGTGGA-3′
Col1a1a forward primer	5′-TAGCCCCTATGGACGTTGGT-3′
Col1a1a reverse primer	5′-CGCAGGTCTAAGCAAGTGGA-3′
Col1a1b forward primer	5′-TGGCATGACCGGCCCTATTG-3′
Col1a1b reverse primer	5′-CTCTCCTTTAGCACCAGGCTGT-3′
Col1a2 forward primer	5′-GAGGCCAGCCTGGTAACATT-3′
Col1a2 reverse primer	5′-GTTACCATCAGGACCAGGGC-3′
Elastin1 forward primer	5′-AAAACCAGGTTACGGCTCTGT-3′
Elastin1 reverse primer	5′-TCCTCCTGGATAAGCTCCGTATC-3′

Table 1. Primer sequence for PCR.

Liposomes	Size in diameter/nm	Polydispersity Index	Zeta potential/mV	Encapsulation efficiency/%
EA-L	149.97 ± 1.80	0.294 ± 0.01	− 3.47 ± 0.20	84.51 ± 0.88
EA-HA0.8 k-L	135.61 ± 1.56	0.273 ± 0.01	− 5.34 ± 0.13	88.71 ± 1.23
EA-HA5k-L	140.30 ± 1.30	0.291 ± 0.01	− 5.67 ± 0.09	91.16 ± 3.06
EA-HA52k-L	158.73 ± 1.91	0.297 ± 0.01	− 5.53 ± 0.21	86.93 ± 1.07

Table 2. Characteristics of EA-loaded liposomes (n = 3).

Statistical analysis

All experiments were done in triplicate, and the results were reported as mean ± standard deviation (SD). The GraphPad Prism version 8.0.2 was used to analyze obtained data, and the comparisons were evaluated using one-way ANOVA and Student's t-test with P value < 0.05 considered significance level.

Results and discussion

Preparation and characterization of EA-HA-L

Studies have shown that low molecular weight HA has a better transdermal penetration effect than high molecular weight HA[19]. However, it is still unclear how low the molecular weight of HA is required to deliver drugs to deeper dermis layers. Therefore, in order to overcome the natural skin barrier and deliver EA to the dermis, where collagen and elastin are highly expressed, we first chemically linked different molecular weights (0.8 kDa, 5 kDa and 52 kDa) of oligomeric HA to cholesterol (HA-Chol), and then used them to fabricate a novel liposome-based transdermal nanosystem for the delivery of EA. Due to the enhanced hydrophilicity of cholesterol through modification with oligomeric HA, HA-Chol was dissolved in water instead of organic solvent to hydrate the lipid thin-films formed by EA and SPC, which was different from the traditional thin-film dispersion method for preparing liposomes. The physicochemical properties of EA-HA-L with different molecular weights of oligomeric HA are shown in Table 2. It can be found that the particle sizes of EA-HA-L increased with the increase of molecular weight of HA, but all were less than 200 nm, which was beneficial for transdermal drug delivery[20]. The Zeta potentials of EA-HA-L were about -5 mV, and there was no significant change with the increase in molecular weight of oligomeric HA. However, the Zeta potentials of EA-HA-L were all higher than those of EA-L, which might be related to the superposition of the negative charge of HA. Importantly, the encapsulation efficiencies of EA-HA-L all exceeded 85%, higher than that of EA-L, while the polydispersity indexes were all below 0.3, implying that these three molecular weights of oligomeric HA-modified liposomes had successfully entrapped EA, with high EA encapsulation efficiency and relatively uniform particle size.

Skin penetration and retention of EA

In order to elucidate the effect of oligomeric HA molecular weight on transdermal delivery of EA, we first carried out skin penetration and retention experiments by simulating human skin with SD rat abdominal skin. The results are shown in Fig. 2. The cumulative permeation amount of EA within 24 h in each experimental group increased with the prolongation of permeation time (Fig. 2a). Due to the low LogP value of EA, it is very difficult for free EA to break through the stratum corneum barrier, so the cumulative permeation amount of the free EA group after 24 h was only 28.50 ± 3.43 μg/cm^2, significantly lower than that of EA-L group (P < 0.05). Meanwhile, the cumulative skin retention amount of EA in the free EA group after 24 h was also markedly lower than that of the EA-L group (Fig. 2b, P P < 0.0001), showing that the conventional liposomes without any modification facilitated the transdermal delivery of EA. Xu and Cai et al. prepared ibuprofen-loaded conventional liposomes (IBU-LP) and found that IBU-LP improved drug penetration and retention in the skin. This may be due to the similarity between the composition of IBU-LP and skin lipid structure, as well as the presence of phospholipids, which have good compatibility and affinity for the skin, allowing more IBU to remain in the skin[21,22]. Remarkably, compared to the EA-L group, the three oligomeric HA-modified liposome groups exhibited higher skin permeation rates. Their 24-h accumulative penetration and retention amounts exceeded

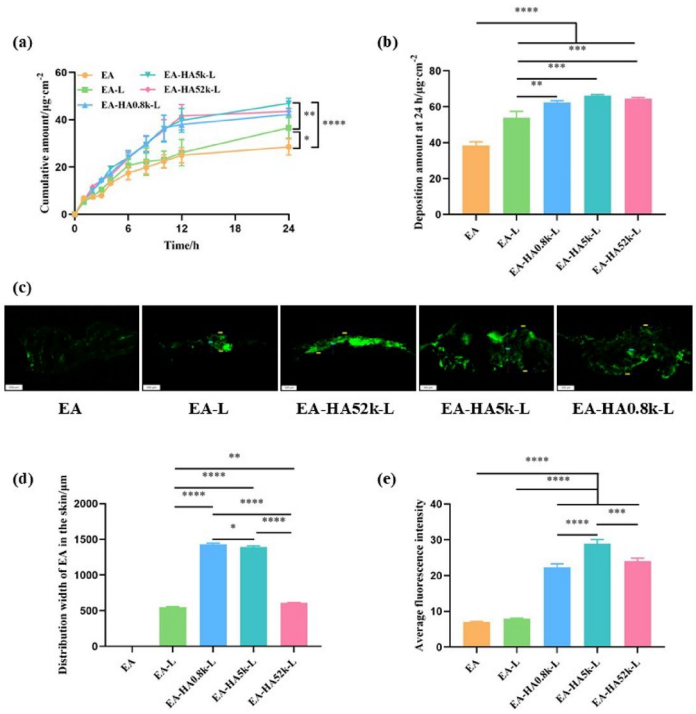

Fig. 2. (**a**) The cumulative permeation amount of EA in rat skin after incubation with different EA formulations at different times. (**b**) The deposition amount of EA in rat skin after incubation with different EA formulations for 24 h. (**c**) CLSM images of rat skin after treatment with different EA formulations for 24 h. The white lines in each image represented the highest and lowest points of the fluorescent band to estimate the penetration depth of EA. (**d**) The distribution width analysis of EA is according to the distance between the highest and lowest points of the fluorescent band. (**e**) The fluorescence intensity analysis is based on fluorescent bands in CLSM images. $^{*}P<0.05$, $^{**}P<0.01$, $^{***}P<0.001$, $^{****}P<0.0001$.

40 μg/cm^2 and 60 μg/cm^2, respectively. Among them, EA-HA5k-L brought about the best-promoting effect on drug penetration, and its 24-h cumulative drug penetration amount was 1.28 times that of EA-L ($P<0.01$) and 1.65 times that of free EA ($P<0.0001$). At the same time, its 24-h drug retention amount was 1.23 times higher than that of EA-L ($P<0.001$) and 1.72 times that of free EA ($P<0.0001$). Xie and Ji prepared HA (150 kDa)-containing ethosomes for transdermic delivery of rhodamine B (HA-ES-RB). Similar to our results, HA-ES-RB also showed a better penetration effect than ES-RB without HA[23].

Distribution of EA in the skin

Although 5 kDa of HA-modified liposomes displayed the highest accumulated penetration and retention of EA, there was no significant difference compared to the other two molecular weight HA-modified liposomes. Therefore, in order to further explicit the molecular weight of oligomeric HA corresponding to the best transdermal effects, we utilized the green fluorescence properties of EA itself to observe the distribution of EA in the skin via laser scanning confocal technique[24]. As shown in Fig. 2c, except for the free EA group, the other four liposome groups appeared with obvious green fluorescence of EA in the skin after 24 h of incubation. In particular, the three EA-HA-L groups exhibited wider and brighter fluorescent bands representing EA, showing extremely significant differences in fluorescent intensity compared to the free EA and EA-L groups (Fig. 2e, $P<0.0001$). Consistent with the previous drug penetration results, the EA-HA5k-L group presented the highest fluorescent intensity, with evident differences compared with EA-HA52k-L ($P<0.001$) and EA-HA0.8 k-L ($P<0.0001$). According to the highest and lowest points of the fluorescent band marked by white lines in Fig. 2d, the distribution width of EA in the EA-HA52k-L group was estimated to be about 600 μm, close to 550 μm of EA-L. However, the distribution width of EA-HA5k-L and EA-HA0.8k-L unexpectedly exceeded 1000 μm, surpassing the epidermal layer thickness[25], proving that both 5 kDa and 0.8 kDa of HA have the potential to deliver EA to the dermis. Ni and Zhang observed the distribution of HA labelled with fluorescent dye FITC in the skin and found that HA with molecular weights of 5 kDa and 8 kDa could pass through the stratum corneum, while HA above 8 kDa just stayed on the stratum corneum. Notably, our results directly showed that HA with a molecular weight of less than 5 kDa could also overcome the stratum corneum barrier and deliver drugs into the dermis. Although the distribution width of EA-HA0.8k-L was larger than that of EA-HA5k-L ($P<0.05$), its fluorescent intensity was significantly weaker than that of EA-HA5k-L ($P<0.0001$), implying that EA-HA5k-L held the optimal transdermal promotion effect. Hence, EA-HA5k-L was chosen for further research, including drug release behaviour, transdermal mechanism, skin irritation, anti-ageing effect, and so on.

Microscopic morphology and drug release behaviour of EA-HA5k-L

As shown in Fig. 3a,b, the micromorphology of EA-L and EA-HA5k-L was witnessed by TEM as a uniform-sized sphere. Due to the presence of acidic substances such as urea, salts, amino acids and free fatty acids on the surface of human skin, the cutaneous surface is usually weakly acidic, and the pH of normal skin is usually between 5.0 and 5.6[26,27], so we chose a buffer solution with a pH of 5.5 to simulate the skin microenvironment and evaluate EA release behaviour of EA-HA5k-L. As shown in Fig. 3c,d, free EA exhibited a rapid release behaviour in a pH 7.4 release environment, with an accumulative release of nearly 100% within 6 h. However, at pH 5.5, the accumulative release of free EA within 6 h was only 55%, and after 24 h, it approached 100%. This might be because EA was essentially acidic and dissolved slower under acidic conditions than under neutral conditions. After being entrapped by conventional liposomes and HA-modified liposomes, the release rate of EA slowed down at pH 5.5 and pH 7.4, exhibiting sustained slow-release behaviour. Under these two pH conditions, the 12-h accumulative release amount of EA-HA5k-L group was both less than 50%, lower than that of EA-L, indicating that HA modification retarded the release of EA. Meanwhile, like free EA, the release behaviour of EA-HA5k-L was also affected by pH, and the release rate of 1 h was 12.31% at pH 5.5 but 36.71% at pH 7.4. In addition, EA-HA5k-L had specific low-temperature storage stability, and there were no apparent changes in particle size and EE when stored at 4 °C for 14 days (supplementary Fig. S2).

Transdermal mechanism study of EA-HA5k-L

The stratum corneum is a multilayered dense membrane structure composed of keratinocytes and interstitial lipids, which forms a primary natural barrier for exogenous substances, including most drugs, so we first observed the ultrastructure of the stratum corneum. As expected, the stratum corneum surface of the control group was relatively smooth and dense (Fig. 4a). There were no obvious gaps between the layers of the epidermis (Fig. 4b). But after treatment with EA, EA-L and EA-HA5k-L, the surface of the stratum corneum became rough and loose, with many wrinkles. There were obvious clefts and gaps between the epidermis layers, especially in the EA-HA5k-L group, where the interlayer gap was the largest. Similar phenomena also appeared in the HE-stained skin tissue sections. The stratum corneum in the EA-HA5k-L group was loose, hollow, and partially detached, distinctly different from the tight stratum corneum in the control group and the thickened stratum corneum in the EA-L group (Fig. 4c), further testifying that EA-HA5k-L could readily disrupt the tight structure of the stratum corneum owing to its hydration effect and intense interaction with keratin and lipids proven by previous researchers[28].

E-cadherin is a crucial intercellular junction protein that maintains cell morphology, motility and adhesion[29,30]. In the skin, it is mainly expressed in the viable epidermis, such as the spinous and basal layers, the second natural barrier for drug transdermal permeation. So, its downregulation will cause weakened intercellular adhesion and amplified skin permeability, making it easier for drugs to penetrate the skin's deeper layers[31,32]. Immunohistochemical analysis showed that the expression of e-cadherin in the epidermal layer of the EA-HA5k-L group obviously declined compared with the control group (Fig. 4d), indicating that EA-HA5k-L could effectively open the tight junctions of epithelial cells in the viable epidermis, thereby boosting penetration through paracellular pathway, which is one of the main pathways for drug penetration.

Skin irritation test of EA-HA5k-L

As a classical method for predicting eye irritation, the HET-CAM is also commonly used for in vitro skin irritation assessment of cosmetic products[16]. After exposing 1% SDS to the CAM surface, vascular bleeding was immediately observed, and coagulation spots occurred 300 s later (Fig. 5). Based on these vascular injury phenomena, the irritation index of 1% SDS as positive control was judged to be 18.26, showing a solid irritation

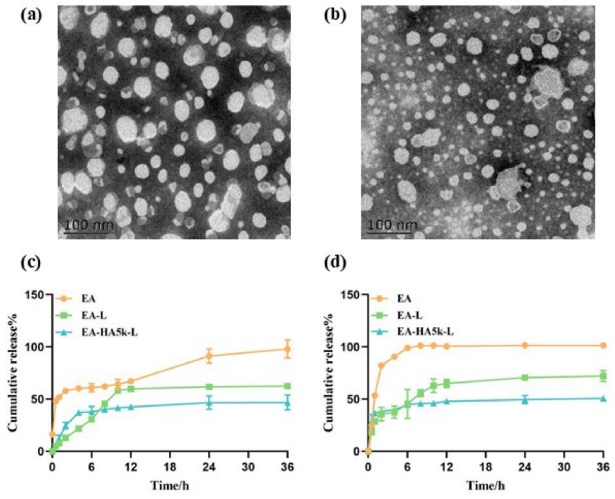

Fig. 3. TEM images of EA-L (**a**) and EA-HA5k-L (**b**). The release behaviours of EA, EA-L and EA-HA5k-L at pH 5.5 (**c**) and pH 7.4 (**d**).

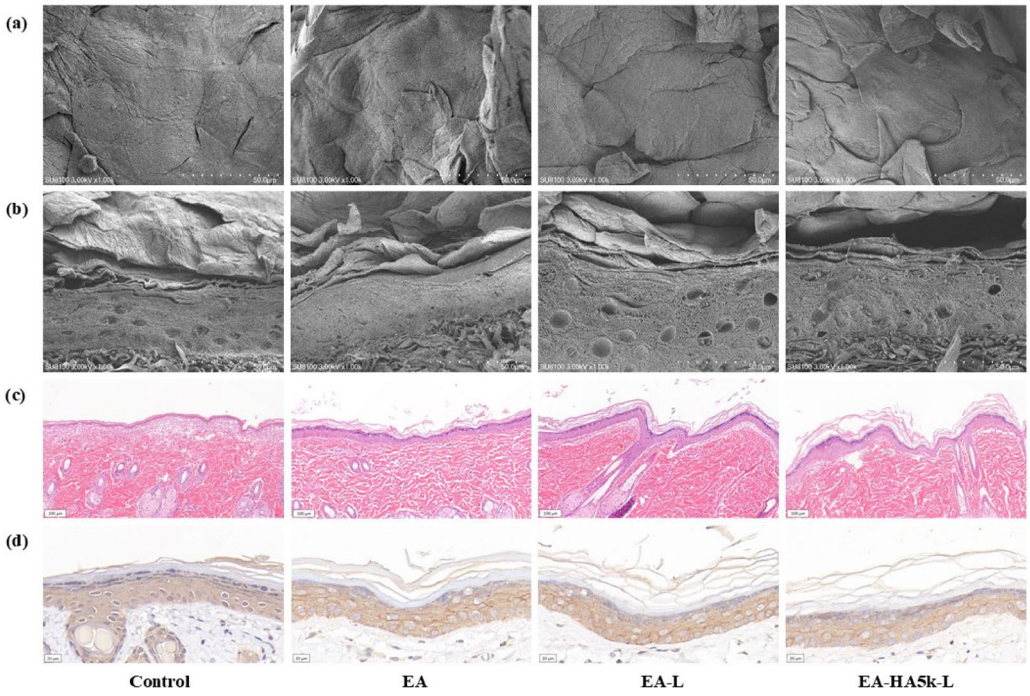

Fig. 4. Cross-sectional (**a**) and longitudinal morphology (**b**) of rat skin after treatment with saline, EA, EA-L, and EA-HA5k-L for 12 h, respectively. (**c**) H&E staining of rat skin (scale bars: 100 μm). (**d**) Immunohistochemical analysis of e-cadherin in rat skin (scale bars: 20 μm).

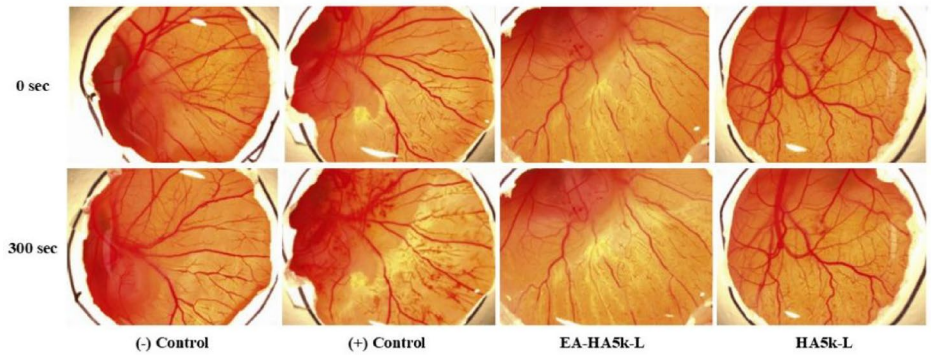

Fig. 5. Irritating responses of CAM surface after treatment with different samples for 300 s. (−) control was 0.9% NaCl, and (+) control was 1% SDS.

potential to skin tissue. However, after the dropwise addition of EA-HA5k-L, there was not any obvious vascular damage appeared on the CAM surface even after 300 s, similar to the phenomena observed in the negative control group of 0.9% NaCl and HA5k-L group. The irritation index of EA-HA5k-L was only 0.04, so it can be considered that EA-HA5k-L has no skin irritation and is safe for dermal administration. Also, HA5k-L, with an irritation index of 0.08, is nonirritating to the skin and can be used as a nanocarrier for drug transdermal delivery. The irritation index of different formulations are listed in Table 3.

In vitro antioxidant activity of EA-HA5k-L

Free radicals are constantly produced in the metabolic process of the human body, and the natural antioxidant defence system continuously neutralizes these new free radicals to achieve a balance of free radicals, but excessive free radicals can aggravate ageing and trigger a series of diseases[33]. DPPH radical, discovered one hundred years ago, is a stable nitrogen synthetic radical that widely used to determine the antioxidant activities of foods and fruit extracts[34]. Hydroxyl radicals are an important reactive oxygen species that trigger oxidative reactions and damage the structure of collagen, making it fragile and prone to breakage. Over time, the degradation of collagen leads to signs of ageing, such as wrinkles and sagging skin[35].

Formulation	Irritation index	Classification
1% SDS	18.26	Irritating
0.9% NaCl	0.00	Nonirritating
EA-HA5k-L	0.04	Nonirritating
HA5k-L	0.08	Nonirritating

Table 3. The irritation index of positive control (1% SDS), negative control (0.9% NaCl), EA-HA5k-L and HA5k-L.

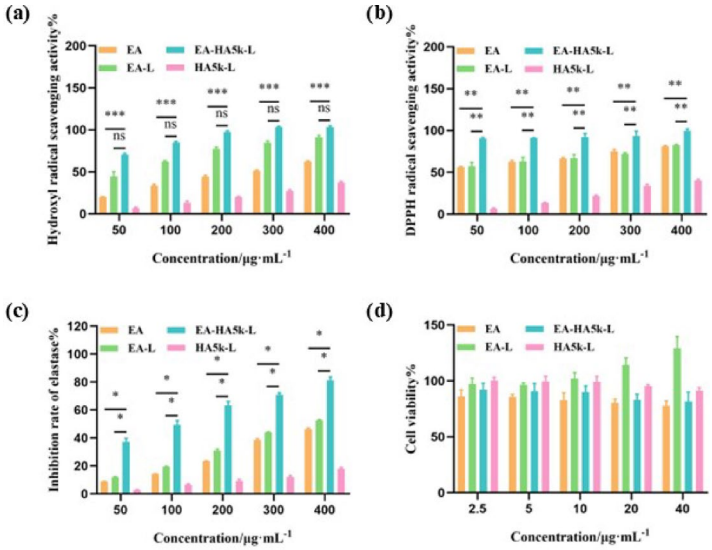

Fig. 6. (**a**) Hydroxyl radical scavenging activities of EA, EA-L, EA-HA5k-L and HA5k-L. (**b**) DPPH radical scavenging activities of EA, EA-L, EA-HA5k-L and HA5k-L. (**c**) In vitro inhibition of elastase enzymes by EA, EA-L, EA-HA5k-L and HA5k-L. (**d**) Cell viability of HDFs after treatment with EA, EA-L, EA-HA5k-L and HA5k-L. $^{*}P<0.05$, $^{**}P<0.01$, $^{***}P<0.001$.

Hence, these two types of free radicals were adopted to investigate the antioxidant activity of EA-HA5k-L. As shown in Fig. 6a, the scavenging effect of each group on hydroxyl radicals enhanced with the increase of the administered concentration. At the same concentration, the scavenging activity of EA-HA5k-L against hydroxyl radicals was significantly higher than that of EA ($P<0.001$), but there was no significant difference compared to EA-L. Differently, at all measured concentrations of EA, the scavenging activity of EA-HA5k-L against DPPH radicals showed a significant difference compared to EA and EA-L ($P<0.01$) (Fig. 6b). Likewise, HA5k-L also displayed a certain hydroxyl and DPPH radicals removing activity at different concentrations, similar to previous reports[36], indicating that the more vital radical scavenging ability of EA-HA5k-L compared to EA-L might result from the endowments of HA.

In vitro elastase inhibition activity

Elastase, a highly selective and specific proteolytic enzyme, catalyzes the hydrolysis of many amino acids to break down elastin[37]. Therefore, inhibiting elastase activity can effectively slow down the degradation of elastin, prevent the formation of wrinkles caused by photoaging and postpone skin ageing. The results of the in vitro elastase inhibition experiment showed that the inhibitory effect of each group, including HA5k-L on elastase, was dose-dependent, and the inhibition rate of EA-HA5k-L was higher than that of EA and EA-L ($P<0.05$) at the same concentration (Fig. 6c), indicating that EA-HA5k-L exerted the most potent inhibitory effect on elastase.

Cell viability assay

In order to confirm the suitable cell administration concentration, we first assessed the cytotoxicity of different EA formulations on HDFs at different concentrations, and the result is shown in Fig. 6d. Within the measured concentration range, the cell viability of blank liposomes HA5k-L was above 90%, indicating that HA5k-L had a certain biosafety. Except for EA-L, the cell activities of free EA and EA-HA5k-L decreased with increasing EA concentration. When the EA concentration was 40 μg/mL, above 80% of cells survived in the three EA formulation groups, so 40 μg/mL was chosen as the optimal cell administration concentration for subsequent experiments.

Cellular uptake

CD44 receptors, highly expressed in the epidermal keratinocytes and dermal fibroblasts, have a specific affinity to HA[38,39]. To test whether HA is responsible for the cellular uptake of EA, HDFs were preincubated with HA for 1 h before incubation with different EA formulations. As shown in Fig. 7a–c, when HDFs were not pre-treated with HA, the intracellular fluorescence intensity of EA-HA5k-L was remarkably higher than that of EA and EA-L group, showing that HA-modified liposomes contributed to improving the cellular uptake of EA. However, after HA-pretreatment, the intracellular fluorescence intensity of EA-HA5k-L dramatically decreased, producing a significant difference from non-pretreatment ($P<0.0001$). In stark contrast, HA pretreatment did not cause a decrease in the intracellular fluorescent intensity in the EA and EA-L groups. These results consistently implied that the higher drug uptake in EA-HA5k-L might be associated with CD44-mediated endocytosis. Besides, combining the previous results, it can be inferred that specific recognition of CD44 receptors to HA may facilitate the transmission of EA to the dermis, which is also supported by Ni's research findings[19].

Anti-photoaging effect on human dermal fibroblasts

In addition to age and genetic factors, ultraviolet radiation is a crucial trigger for skin ageing[40]. Ultraviolet radiation, especially UVB radiation, will increase the activity of matrix metalloproteinases 1 (MMP-1), which can decompose collagen and elastin, thereby decreasing the content of collagen and elastin in the dermis and ultimately leading to skin wrinkles[41]. Hence, we surveyed whether HDFs could resist the increase of MMP-1 and the decrease of collagen caused by UVB irradiation after incubation with different EA formulations.

As displayed in Fig. 7d, the MMP-1 content of the model group increased sharply after HDFs were radiated by UVB, showing an extremely significant difference from the control group ($P<0.0001$). However, after incubation with three EA formulations before UVB radiation, the MMP-1 content in HDFs evidently declined, suggesting that free EA, EA-L and EA-HA5k-L effectively inhibited the increase of MMP-1 induced by UVB irradiation. Surprisingly, the EA-HA5k-L group showed the most significant inhibitory effect on UVB-induced upregulation of MMP-1 content, and the MMP-1 content was significantly lower than that of free EA ($P<0.001$) and EA-L group ($P<0.05$).

Type I collagen is one of the main components of the extracellular matrix of the dermis and can be hydrolyzed by MMP-1. Therefore, we further investigated whether EA-HA5k-L could block the downregulation of type I collagen in HDFs triggered by excessive MMP-1. As seen in Fig. 7e, the type I collagen content in the model group was significantly lower than that of the control group ($P<0.01$), illustrating that the UVB irradiation successfully detonated a decrease in type I collagen content, one of the markers of cellular ageing. As expected, the content of type I collagen in HDFs obviously increased after incubation with EA, EA-L and EA-HA5k-L, among which EA-HA5k-L aroused the highest increase in the type I collagen content due to the most vigorous

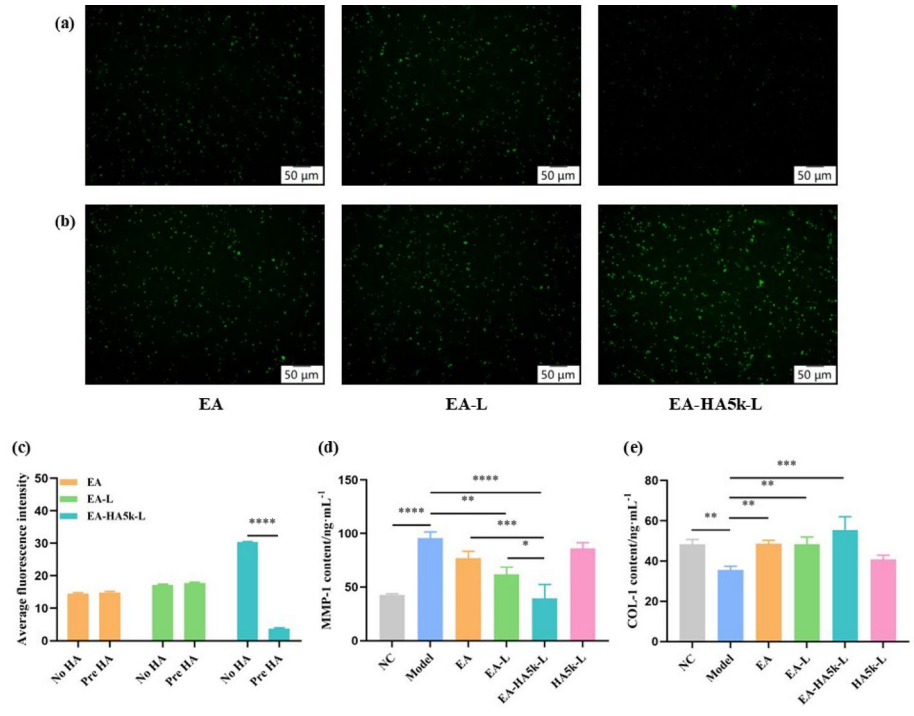

Fig. 7. CLSM images of EA uptake by HDFs incubated with different EA formulations for 4 h with (**a**)/without (**b**) 1 h of HA-pretreatment. (**c**) Mean fluorescence intensity analysis in HDFs incubated with different EA formulations for 4 h under 1 h of HA-pretreatment or non-pretreatment. (**d**) The content of MMP-1 in HDFs incubated with EA, EA-L, EA-HA5k-L or HA5k-L and then irradiated with UVB. (**e**) The content of type I collagen in HDFs incubated with EA, EA-L, EA-HA5k-L or HA5k-L and then irradiated with UVB. $^{*}P<0.05$, $^{**}P<0.01$, $^{***}P<0.001$, $^{****}P<0.0001$.

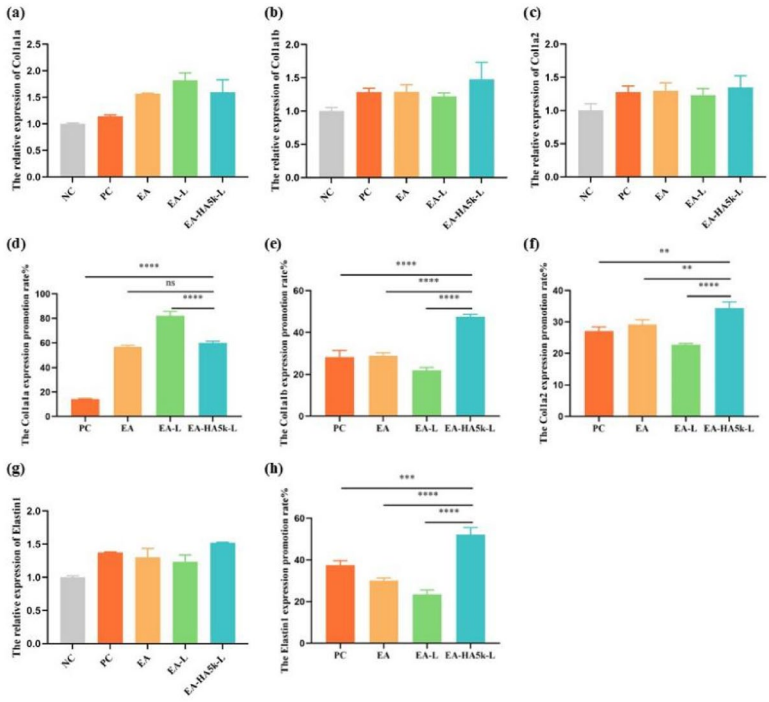

Fig. 8. The relative expression and expression promotion rate of Type I collagen and elastin genes in zebrafish after treatment with different formulations for 24 h. $^{**}P<0.01$, $^{***}P<0.001$, $^{****}P<0.0001$.

resistance to UVB-induced upregulation of MMP-1. Similar to the result of MMP-1 content, HA5k-L also did not show apparent inhibition to the downregulation of type I collagen induced by UVB, indicating the dominant effect of EA on anti-photoaging. According to these results, it is reasonable to conclude that HA-modified liposomes effectively prevented the loss of type I collagen induced by UVB and had the ability to improve the anti-photo ageing effectiveness of EA, which might be related to the increasing cellular uptake of EA-mediated by CD44 receptors.

Zebrafish experiment

The cutaneous structure of zebrafish is analogous to that of humans, and the regulatory pathways for type I collagen and elastin are also similar[42], so we chose zebrafish as an animal model to testify to the effect of EA-HA5k-L on the gene expression of type I collagen and elastin. No death or deformity was observed in the free EA group at concentrations of 2.5 g/L or below (supplementary Table S1), which meant that the MTC of the free EA group was 2.5 g/L. However, the MTC of EA-L and EA-HA5k-L groups raised to 10.0 g/L (supplementary Table S2–3), which might be because biocompatible materials SPC and HA alleviated the toxicity of EA, so the final dosage for each experimental group was assigned to 2.5 g/L. Additionally, acetyl hexapeptide-8, a biomimetic peptide that inhibits neurotransmitters, was selected as a positive drug due to its antiwrinkle and anti-ageing effects comparable to botulinum toxin.

They were considering that there are three types of type I collagen genes in zebrafish bodies, namely col1a1a, col1a1b, and col1a2[43], the relative expression of these three genes in zebrafish was detected. The expression promotion rate was also calculated after incubation with the same dose of different EA formulations and acetyl hexapeptide-8. As shown in Fig. 8, compared with the control group, all administration groups could upregulate the expression of three types of type I collagen genes in zebrafish. The expression promotion rate of col1a1a in the EA-HA5k-L group was 59.86%, which was dramatically lower than the EA-L group ($P<0.0001$) and had no significant difference from the free EA group but significantly higher than the positive control group ($P<0.0001$). Meanwhile, EA-HA5k-L showed the most substantial promotion effect on the expression of col1a1b gene, and its expression promotion rate was remarkably higher than that of free EA ($P<0.0001$), EA-L ($P<0.0001$) and positive control groups ($P<0.0001$), which was similar to the expression results of col1a2 gene. Besides, EA-HA5k-L also upregulated the expression of elastin in zebrafish, and its expression promotion rate showed prominent differences compared to other groups. These results indicated that EA-HA5k-L played a better role in preventing zebrafish from ageing by promoting the expression of type I collagen and elastin genes.

Conclusion

In this study, based on the difficulty of EA breaking through the dense stratum corneum and the fact that low molecular weight HA can promote drug skin penetration, we fabricated a liposome-based nanocarrier via oligomeric HA-modified cholesterol to achieve dermal delivery of EA. Moreover, we elucidated that the molecular weight of HA had an essential effect on dermal delivery of EA. 5 kDa of HA could exert the best

skin penetration efficacy and deliver EA to the dermis, which might depend on the looseness of the stratum corneum and reduction of e-cadherin caused by HA, as well as the specific recognition of CD44 receptor to HA. Even liposomes modified with 0.8 kDa of HA also could widely deliver EA to the dermis, while it was difficult for 52 kDa of HA to deliver EA to the dermis. Overall, EA-HA5k-L, characterized by good stability and low irritation, is an effective dermal delivery system that can elevate the anti-ageing effect of EA and potentially polish up the application prospects of natural polyphenols EA in cosmetics.

Data availability

Data is provided within the manuscript or supplementary information files.

Received: 12 February 2025; Accepted: 11 June 2025
Published online: 26 July 2025

References

1. Yang, Y. et al. Injectable self-healing bioactive antioxidative one-component poly(salicylic acid) hydrogel with strong ultraviolet-shielding for preventing skin light injury. *Mater. Sci. Eng. C Mater. Biol. Appl.* **126**, 112107 (2021).
2. Couteau, C., Cheignon, C., Paparis, E. & Coiffard, L. J. Silymarin, a molecule of interest for topical photoprotection. *Nat. Prod. Res.* **26**, 2211 (2012).
3. Kikuchi, H., Harata, K., Madhyastha, H. & Kuribayashi, F. Ellagic acid and its fermentative derivative urolithin A show reverse effects on the gp91-phox gene expression, resulting in opposite alterations in all-trans retinoic acid-induced superoxide generating activity of U937 cells. *Biochem. Biophys. Rep.* **25**, 100891 (2021).
4. Wang, W. et al. Ellagic acid: A dietary-derived phenolic compound for drug discovery in mild cognitive impairment. *Front. Aging Neurosci.* **14**, 925855 (2022).
5. Harper, P. A review of the dietary intake, bioavailability and health benefits of ellagic acid (EA) with a primary focus on its anti-cancer properties. *Cureus* **15**, e43156 (2023).
6. Ortiz-Ruiz, C. V., Berna, J., Tudela, J., Varon, R. & Garcia-Canovas, F. Action of ellagic acid on the melanin biosynthesis pathway. *J. Dermatol. Sci.* **82**, 115 (2016).
7. Sharifi-Rad, J. et al. Ellagic acid: A review on its natural sources, chemical stability, and therapeutic potential. *Oxid. Med. Cell Longev* **2022**, 3848084 (2022).
8. Nyamba, I., Lechanteur, A., Semde, R. & Evrard, B. Physical formulation approaches for improving aqueous solubility and bioavailability of ellagic acid: A review. *Eur. J. Pharm. Biopharm.* **159**, 198 (2021).
9. Jung, S. H. et al. Topical application of liposomal cobalamin hydrogel for atopic dermatitis therapy. *Pharmazie* **66**, 430 (2011).
10. Vovesna, A., Zhigunov, A., Balouch, M. & Zbytovska, J. Ceramide liposomes for skin barrier recovery: A novel formulation based on natural skin lipids. *Int. J. Pharm.* **596**, 120264 (2021).
11. Carita, A. C. et al. Elastic cationic liposomes for vitamin C delivery: Development, characterization and skin absorption study. *Int. J. Pharm.* **638**, 122897 (2023).
12. Akram, M. W. et al. Transfersomes: A revolutionary nanosystem for efficient transdermal drug delivery. *AAPS PharmSci. Tech.* **23**, 7 (2021).
13. Xiao, S. et al. The development and evaluation of hyaluronic acid coated mitochondrial targeting liposomes for celastrol delivery. *Drug Deliv.* **30**, 2162156 (2023).
14. Hu, J. et al. Gut microbiota-derived 3-phenylpropionic acid promotes intestinal epithelial barrier function via AhR signaling. *Microbiome* **11**, 102 (2023).
15. Yang, R. M. et al. Myeloid cells interact with a subset of thyrocytes to promote their migration and follicle formation through NF-kappaB. *Nat. Commun.* **14**, 8082 (2023).
16. Hsieh, W. C. et al. Improved skin permeability and whitening effect of catechin-loaded transfersomes through topical delivery. *Int. J. Pharm.* **607**, 121030 (2021).
17. Lee, S. E. et al. Anti-photoaging and anti-oxidative activities of natural killer cell conditioned medium following UV-B irradiation of human dermal fibroblasts and a reconstructed skin model. *Int. J. Mol. Med.* **44**, 1641 (2019).
18. Xu, F. W. et al. Beneficial effects of green tea EGCG on skin wound healing: A comprehensive review. *Molecules* **26** (2021).
19. Ni, C. et al. Hyaluronic acid and HA-modified cationic liposomes for promoting skin penetration and retention. *J. Control Release* **357**, 432 (2023).
20. Kalave, S., Chatterjee, B., Shah, P. & Misra, A. Transdermal delivery of macromolecules using nano lipid carriers. *Curr. Pharm. Des.* **27**, 4330 (2021).
21. Mota, A. C. et al. In vivo and in vitro evaluation of octyl methoxycinnamate liposomes. *Int. J. Nanomed.* **8**, 4689 (2013).
22. Xu, Y. et al. Liposome and microemulsion loaded with ibuprofen: From preparation to mechanism of drug transport. *J. Microencapsul.* **39**, 539 (2022).
23. Xie, J., Ji, Y., Xue, W., Ma, D. & Hu, Y. Hyaluronic acid-containing ethosomes as a potential carrier for transdermal drug delivery. *Colloids Surf. B Biointerfaces* **172**, 323 (2018).
24. Najafi, A. et al. Improvement of post-thawed sperm quality in broiler breeder roosters by ellagic acid-loaded liposomes. *Poult. Sci.* **98**, 440 (2019).
25. Sapkota, R. & Dash, A. K. Liposomes and transferosomes: A breakthrough in topical and transdermal delivery. *Ther. Deliv.* **12**, 145 (2021).
26. Ali, S. M. & Yosipovitch, G. Skin pH: From basic science to basic skin care. *Acta Derm. Venereol.* **93**, 261 (2013).
27. Bigliardi, P. L. Role of skin pH in psoriasis. *Curr. Probl. Dermatol.* **54**, 108 (2018).
28. Witting, M. et al. Interactions of hyaluronic Acid with the skin and implications for the dermal delivery of biomacromolecules. *Mol. Pharm.* **12**, 1391 (2015).
29. van Roy, F. & Berx, G. The cell-cell adhesion molecule E-cadherin. *Cell Mol. Life Sci.* **65**, 3756 (2008).
30. Daulagala, A. C., Bridges, M. C. & Kourtidis, A. E-cadherin beyond structure: A signaling hub in colon homeostasis and disease. *Int. J. Mol. Sci.* **20** (2019).
31. Wato, K. et al. An insight into the role of barrier related skin proteins. *Int. J. Pharm.* **427**, 293 (2012).
32. Choi, J. H. et al. Treatment with low-temperature atmospheric pressure plasma enhances cutaneous delivery of epidermal growth factor by regulating E-cadherin-mediated cell junctions. *Arch. Dermatol. Res.* **306**, 635 (2014).
33. Liochev, S. I. Reactive oxygen species and the free radical theory of aging. *Free Radic. Biol. Med.* **60**, 1 (2013).
34. Letelier, M. E. et al. DPPH and oxygen free radicals as pro-oxidant of biomolecules. *Toxicol. In Vitro* **22**, 279 (2008).
35. He, X., Wan, F., Su, W. & Xie, W. Research progress on skin aging and active ingredients. *Molecules* **28** (2023).
36. Paiva, W., Medeiros, W., Assis, C. F., Dos, S. E. & de Sousa, J. F. Physicochemical characterization and in vitro antioxidant activity of hyaluronic acid produced by Streptococcus zooepidemicus CCT 7546. *Prep. Biochem. Biotechnol.* **52**, 234 (2022).
37. Imokawa, G. Mechanism of UVB-induced wrinkling of the skin: Paracrine cytokine linkage between keratinocytes and fibroblasts leading to the stimulation of elastase. *J. Investig. Dermatol. Symp. Proc.* **14**, 36 (2009).

38. Yasaka, N., Furue, M. & Tamaki, K. CD44 expression in normal human skin and skin tumors. *J. Dermatol.* **22**, 88 (1995).
39. Kleiser, S. & Nystrom, A. Interplay between cell-surface receptors and extracellular matrix in skin. *Biomolecules* **10** (2020).
40. Liu, T. et al. Oroxylin A ameliorates ultraviolet radiation-induced premature skin aging by regulating oxidative stress via the Sirt1 pathway. *Biomed. Pharmacother.* **171**, 116110 (2024).
41. Lephart, E. D. & Naftolin, F. Menopause and the skin: Old favorites and new innovations in cosmeceuticals for estrogen-deficient skin. *Dermatol. Ther. (Heidelb)* **11**, 53 (2021).
42. Han, J., Gong, R., Wang, B., Gong, T. & Chen, X. Evaluation of the safety and efficacy of cosmetics ingredient Spherulites Paeony Superior Retinol. *J. Cosmet. Dermatol.* (2024).
43. Gistelinck, C. et al. Zebrafish collagen type I: Molecular and biochemical characterization of the major structural protein in bone and skin. *Sci. Rep.* **6**, 21540 (2016).

Acknowledgements
This study was carried out with the kind collaboration of the participants.

Author contributions
X.Y.: Methodology, Resources, Data Curation, Writing – Original Draft. K.M.: Resources, Investigation. Z.C.: Resources, Investigation. Y.M.: Validation, Supervision. J.X.: Funding acquisition. C.C.: Funding acquisition. X.C.: Conceptualization, Supervision, Project administration, Writing – Review & Editing. Z.S.: Conceptualization, Supervision, Project administration, Funding acquisition. All authors reviewed the manuscript.

Funding
This research project was supported by the Hubei Province Key Research and Development Project (2022BCA053) and the University Level Key Project of Traditional Chinese Medicine (2022ZZXZ003 and 2023ZZXJB002).

Declarations

Competing interests
The authors declare no competing interests.

Additional information
Supplementary Information The online version contains supplementary material available at https://doi.org/10.1038/s41598-025-06948-0.

Correspondence and requests for materials should be addressed to C.C., X.C. or Z.S.